

Formation and Characterization of Gold Nanoparticles

by Glenna R. Yu, Hans M. Guo, and Yuanping Chen

ARL-TR-6593

September 2013

NOTICES

Disclaimers

The findings in this report are not to be construed as an official Department of the Army position unless so designated by other authorized documents.

Citation of manufacturer's or trade names does not constitute an official endorsement or approval of the use thereof.

Destroy this report when it is no longer needed. Do not return it to the originator.

Army Research Laboratory

Adelphi, MD 20783-1197

ARL-TR-6593**September 2013**

Formation and Characterization of Gold Nanoparticles

Glenna R. Yu, Hans M. Guo, and Yuanping Chen
Sensors and Electron Devices Directorate, ARL

REPORT DOCUMENTATION PAGE			Form Approved OMB No. 0704-0188		
<p>Public reporting burden for this collection of information is estimated to average 1 hour per response, including the time for reviewing instructions, searching existing data sources, gathering and maintaining the data needed, and completing and reviewing the collection information. Send comments regarding this burden estimate or any other aspect of this collection of information, including suggestions for reducing the burden, to Department of Defense, Washington Headquarters Services, Directorate for Information Operations and Reports (0704-0188), 1215 Jefferson Davis Highway, Suite 1204, Arlington, VA 22202-4302. Respondents should be aware that notwithstanding any other provision of law, no person shall be subject to any penalty for failing to comply with a collection of information if it does not display a currently valid OMB control number.</p> <p>PLEASE DO NOT RETURN YOUR FORM TO THE ABOVE ADDRESS.</p>					
1. REPORT DATE (DD-MM-YYYY) September 2013		2. REPORT TYPE Final		3. DATES COVERED (From - To)	
4. TITLE AND SUBTITLE Formation and Characterization of Gold Nanoparticles			5a. CONTRACT NUMBER		
			5b. GRANT NUMBER		
			5c. PROGRAM ELEMENT NUMBER		
6. AUTHOR(S) Glenna R. Yu, Hans M. Guo, and Yuanping Chen			5d. PROJECT NUMBER		
			5e. TASK NUMBER		
			5f. WORK UNIT NUMBER		
7. PERFORMING ORGANIZATION NAME(S) AND ADDRESS(ES) U.S. Army Research Laboratory ATTN: RDRL-SEE-I 2800 Powder Mill Road Adelphi, MD 20783-1197			8. PERFORMING ORGANIZATION REPORT NUMBER ARL-TR-6593		
9. SPONSORING/MONITORING AGENCY NAME(S) AND ADDRESS(ES)			10. SPONSOR/MONITOR'S ACRONYM(S)		
			11. SPONSOR/MONITOR'S REPORT NUMBER(S)		
12. DISTRIBUTION/AVAILABILITY STATEMENT Approved for public release; distribution unlimited.					
13. SUPPLEMENTARY NOTES					
14. ABSTRACT <p>Nanowires grown via the popular vapor-liquid-solid (VLS) growth mechanism require nanodroplets, most often metal, such as gold, to catalyze the growth. As the size and density of the catalytic nanoparticles are the main parameters that define the properties of the resulting nanowires, controlling the growth of these nanoparticles is of particular importance. In this study, molecular beam epitaxy (MBE) was used to grow the nanoparticles on <100> and <211> silicon substrates. A layer of gold was first evaporated onto the wafer and then annealed at various temperatures and for varying lengths of time. We studied the effect of the thickness of the initial gold layer, annealing temperature, and time on the size and density of the gold nanoparticles. Reflection high energy electron diffraction (RHEED) was used to observe the process in situ; and the size, density, diameter, and height of the nanoparticles were determined by atomic force microscope (AFM) and scanning electron microscope (SEM).</p>					
15. SUBJECT TERMS ZnSeTe, Si, HgCdSe, ZnTe, MBE, LWIR, defects, IR, II-VI, Type-2 SLS					
16. SECURITY CLASSIFICATION OF:			17. LIMITATION OF ABSTRACT UU	18. NUMBER OF PAGES 18	19a. NAME OF RESPONSIBLE PERSON Glenna R. Yu
a. REPORT Unclassified	b. ABSTRACT Unclassified	c. THIS PAGE Unclassified			19b. TELEPHONE NUMBER (Include area code) (301) 394-0951

Contents

List of Figures	iv
List of Tables	iv
1. Introduction	1
1.1 Nanowires.....	1
1.2 Molecular Beam Epitaxy.....	1
1.3 Atomic Force Microscopy and Scanning Electron Microscopy	2
2. Experimental	2
2.1 Wafer Preparation.....	2
2.2 Growth Conditions	3
3. Results and Discussion	4
3.1 Gold Film Thickness	4
3.2 Annealing Temperature	5
3.3 Anneal Time	7
4. Conclusions	8
5. References	9
List of Symbol, Abbreviation, and Acronyms	10
Distribution List	11

List of Figures

Figure 1. Schematic illustration of VLS growth mechanism (3).	2
Figure 2. SEM and AFM images of gold nanoparticles annealed at 580 °C for 10 min and varied thicknesses of the gold films. Growth times were (a) 100 s, (b) 200 s, (c) 400 s, (d) 600 s, and (e) 800 s. The top row of images was taken with the SEM at a magnification of about 220,000 times and a working distance of around 14 mm. The second row of images was taken with the AFM at a sample size of 500 nm x 500 nm and vertical scale of 25 nm, with the corresponding 3-D view below.	4
Figure 3. Densities of the gold particles as a function of the thickness of the initial gold film.	5
Figure 4. Diameters of the gold particles as a function of the thickness of the initial gold film.	5
Figure 5. AFM images of gold nanoparticles with a 100-nm-thick initial layer and annealed for 10 min at varied temperatures. Images were taken with a sample size of 500 nm x 500 nm and vertical scale of 25 nm, with the corresponding 3-D view below.	6
Figure 6. Densities of the gold particles as a function anneal temperature.	6
Figure 7. Diameters of the gold particles as a function anneal temperature.	6
Figure 8. AFM images of gold nanoparticles with a 100-nm-thick initial layer and annealed at 530 °C for various times. Images were taken with a sample size of 500 nm x 500 nm and vertical scale of 25 nm, with the corresponding 3-D view below.	7
Figure 9. Densities of the gold particles as a function annealing time.	7
Figure 10. Diameters of the gold particles as a function annealing time.	8

List of Tables

Table 1. Growth conditions.	3
----------------------------------	---

1. Introduction

1.1 Nanowires

One-dimensional nanowires are of increasing interest due to their nanosize, physical properties, and other applications in opto-electronics. For example, nanowires have already been used in light-emitting diodes and lasers, photodetectors, resonant tunneling diodes, field-effect and single-electron transistors, and biochemical sensors (1). In addition to these applications, nanowires are useful because they can be grown almost dislocation free, due to their nano dimension. The quality of crystalline materials is diminished by dislocations and other defects that invariably form because of the lattice mismatch between the grown material and the substrate. As a result, the goal of a crystal grower is to avoid or reduce the formation and propagation of dislocations during the crystal growth process, which leads to a top portion of the epilayer with a reduced dislocation or defect-free. Therefore, when dislocation-free nanowires nucleated on the substrate merge to form a continuous film, voids are left underneath, which act as sinks for dislocations, allowing other structures to be grown stress-free on top of the nanoengineered buffer layer. Thus, nanowires hold a lot of promise for improving the quality of crystalline materials and mitigating the effect of dislocations, leading to better detector performance.

1.2 Molecular Beam Epitaxy

Compared to other growth methods, molecular beam epitaxy's (MBE) relatively low growth temperature, ultrahigh vacuum, and precise control of beam fluxes reduces impurities and allows for greater control in doping individual nanowires and forming complex junctions (2). Furthermore, various methods of *in situ* observation, such as reflection high-energy electron diffraction (RHEED), are relatively easy to implement in an MBE system.

II-VI nanowires, such as cadmium telluride (CdTe) and zinc telluride (ZnTe), are typically grown by a vapor-liquid-solid (VLS) growth mechanism (figure 1), as first described by Wagner and Ellis (1). In this mechanism, catalytic metal droplets on the substrate surface form liquid eutectics. Gold is typically chosen for the catalyst due to its low eutectic temperature. The lower temperature of the eutectic makes the droplets the preferred site for deposition so that the droplets absorb source atoms until they are supersaturated. Nanowires grow underneath the droplet by precipitation and end with a characteristic metallic droplet at the tip. While the length of the nanowires is controlled by the MBE growth conditions, the diameter and location of the nanowires are determined by the gold droplets. Therefore, controlling the size and density of the gold catalysts is essential to understanding the growth of nanowires. For the purposes of growing nanowires that would eventually merge into a continuous film, we wanted the nanoparticles to be

as large and as close together as possible. We used MBE to grow gold nanoparticles and investigated the influence of the relative thickness of the initial layer of gold, the annealing temperature, and the annealing time on the size, density, diameter, and height of the gold particles.

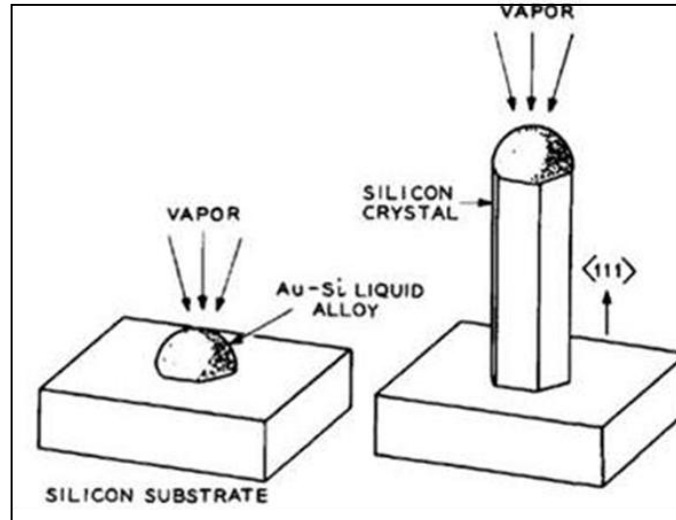


Figure 1. Schematic illustration of VLS growth mechanism (3).

1.3 Atomic Force Microscopy and Scanning Electron Microscopy

Atomic force microscopy (AFM) and scanning electron microscopy (SEM) were both used to characterize these gold nanoparticles due to their high resolution and precise measurement capabilities. Because of the SEM's relatively quick scanning rate, it was used to first confirm that nanoparticles were indeed present, while the AFM was used to provide three-dimensional (3-D) images and the dimensions of the nanoparticles. The SEM contains an electron gun and detectors that interpret the scattering of electrons when the beam interacts with the sample surface. The AFM uses a cantilever with a microscopic sharp-tipped probe that scans the surface of a sample. In tapping mode, the cantilever vibrates at an alterable frequency on the sample. A laser is positioned on the cantilever and the deflections are picked up by photodiodes.

2. Experimental

2.1 Wafer Preparation

The substrates were 3-in silicon (Si) (100) phosphor-doped wafers. They were cleaned by a modified RCA procedure. The wafers were first bathed in a 1:1:5 ammonium hydroxide (NH₃OH): hydrogen peroxide (H₂O₂): water (H₂O) solution to removed organic contaminants and then rinsed with deionized water. They were then bathed in a diluted hydrogen fluoride (HF)

solution to remove a thin silicon dioxide layer followed by a 1:1:5 hydrochloric acid (HCl):H₂O₂:H₂O solution, which was used to remove ionic contaminants. Finally, they were rinsed with deionized water and transferred to the MBE system.

2.2 Growth Conditions

Fabrication of gold particles on Si was conducted using a DCA MBE system equipped with a 3.25-in substrate heater. Three-inch Si(100) nominal wafers were used as substrates. All Si wafers were cleaned using the modified RCA process, as described in section 2.1. This process leaves an approximate 12-Å uniform oxide layer on the Si surface, which must be thermally removed in the growth chamber. For these experiments, the samples were quickly heated to 1050 °C to remove the oxide layer and then quickly cooled under an As₄ flux to 500 °C. Finally, the sample was cooled to the nucleation temperature of 230 °C without any flux. Note, that all temperatures stated are readings from a thermocouple, which was located approximately 10 mm from the back of the substrate. Although the thermocouple does not measure the precise temperature of the sample surface, this configuration provides both excellent temperature control and run-to-run reproducibility. The real substrate temperature was obtained from the calibration based on the melting points of indium (In), selenium (Se), cadmium (Cd), and zinc (Zn). After oxide desorption, a thin gold film was deposited and annealed to form nanoparticles. The temperature of the gold effusion cell was set to 1250 °C for a flux of approximately 0.125 nm/s. The time of deposition, annealing temperature, and annealing time were varied according to table 1. RHEED was used to observe the process *in situ*. After annealing, some samples were studied using SEM and all samples were studied with AFM to look at the size and number density of the particles.

Table 1. Growth conditions.

Estimated Thickness of Initial Au Layer (nm)	Annealing Temperature (°C)	Annealing Time (s)
12.5	580	600
25		
50		
75		
100		
75	480	600
	530	
	580	
	630	
	680	
75	530	300
		600
		900
		1200

3. Results and Discussion

3.1 Gold Film Thickness

The results of varying the thickness of the initial layer of gold can be seen in the SEM and AFM images in figure 2. Extracted densities and diameters of the gold particles were plotted versus the thickness of the initial gold film, as shown in figures 3 and 4, respectively. The 12.5-nm sample did not yield clear nanoparticles and was much flatter than the other samples. The small clusters were densely packed with heights less than 5 nm. The 25-, 75-, and 100-nm samples look mostly similar, but the minimum diameter increases and the range of diameters decreases as thickness increases while the density stays about the same. A critical point occurs around the 50-nm sample, although it may have been a result of leaving it in the MBE chamber overnight because the water cooler broke. Our results seem to indicate that thickness of initial film has a noticeable impact on the minimum diameter of the gold particle and no impact on density and average diameter of the gold particles.

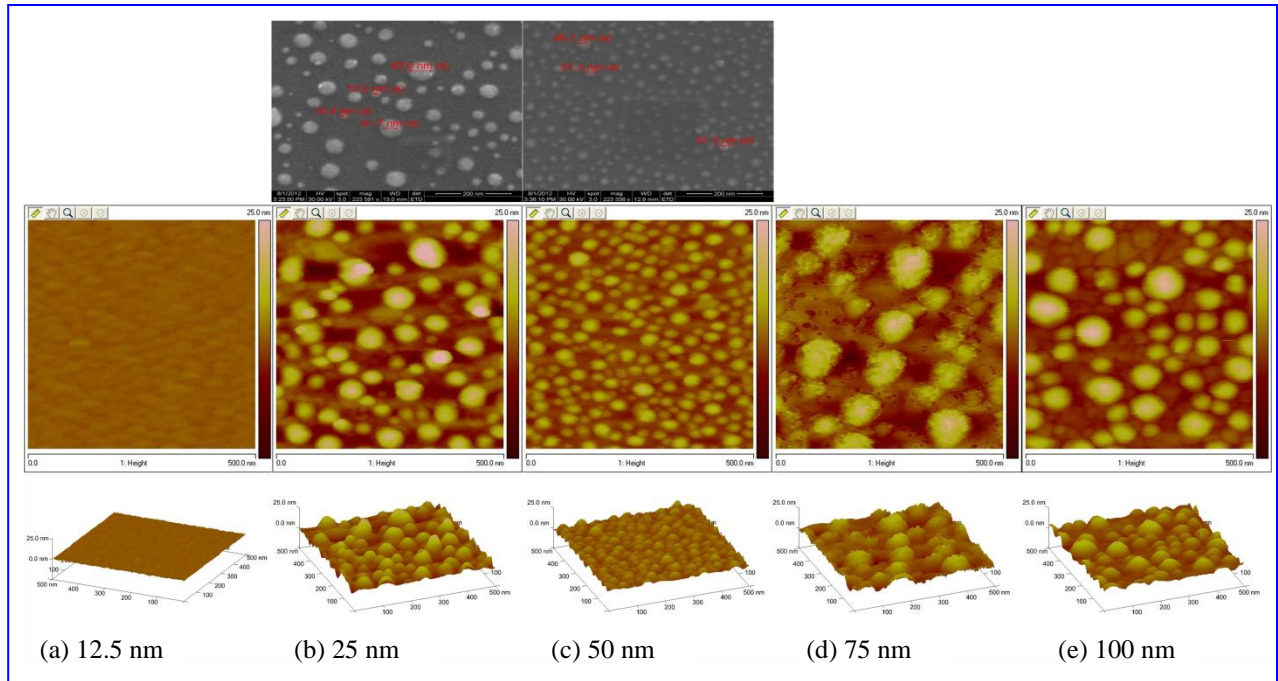


Figure 2. SEM and AFM images of gold nanoparticles annealed at 580 °C for 10 min and varied thicknesses of the gold films. Growth times were (a) 100 s, (b) 200 s, (c) 400 s, (d) 600 s, and (e) 800 s. The top row of images was taken with the SEM at a magnification of about 220,000 times and a working distance of around 14 mm. The second row of images was taken with the AFM at a sample size of 500 nm x 500 nm and vertical scale of 25 nm, with the corresponding 3-D view below.

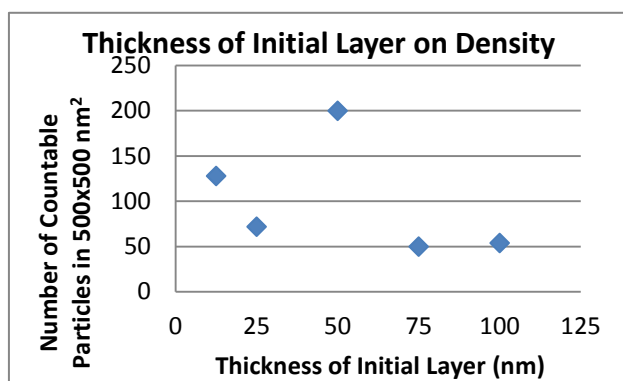


Figure 3. Densities of the gold particles as a function of the thickness of the initial gold film.

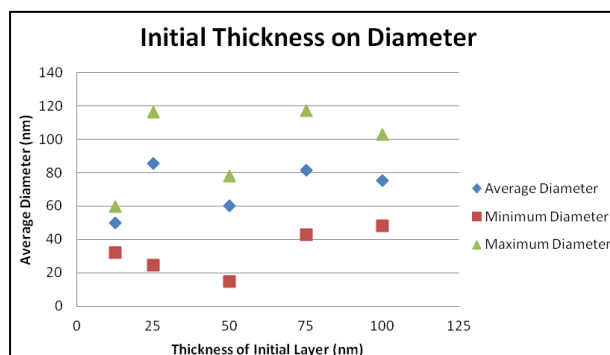


Figure 4. Diameters of the gold particles as a function of the thickness of the initial gold film.

3.2 Annealing Temperature

A 100-nm-thick gold film was annealed at various temperatures to form gold particles. Figure 5 shows the AFM images of the gold particles. Extracted densities and diameters of the gold particles were plotted versus annealing temperatures, as shown in figures 6 and 7, respectively. The results seem to indicate that the annealing temperature does not have a clear effect on the density of the nanoparticles. The minimum diameter appeared to increase slightly as the annealing temperature increased. Annealing at 530 °C yielded the largest nanoparticles, which are best suited for our purposes.

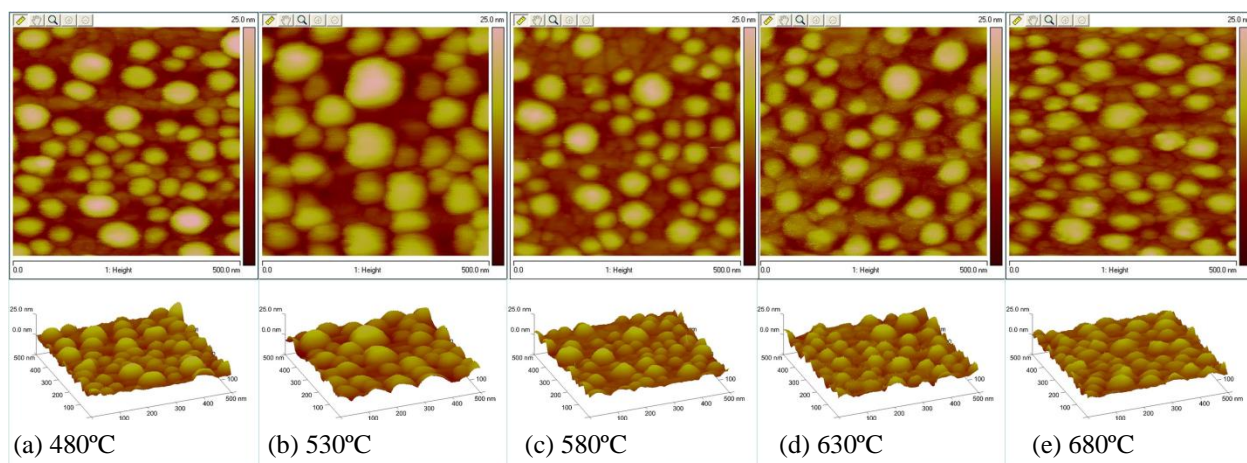


Figure 5. AFM images of gold nanoparticles with a 100-nm-thick initial layer and annealed for 10 min at varied temperatures. Images were taken with a sample size of 500 nm x 500 nm and vertical scale of 25 nm, with the corresponding 3-D view below.

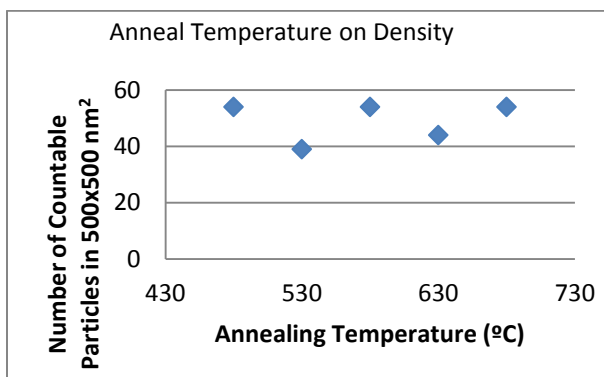


Figure 6. Densities of the gold particles as a function anneal temperature.

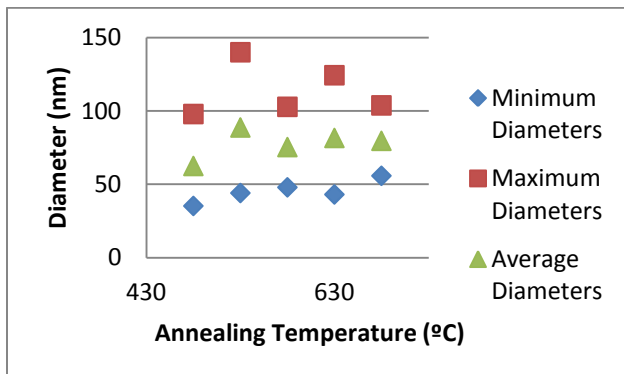


Figure 7. Diameters of the gold particles as a function anneal temperature.

3.3 Anneal Time

AFM images of the gold particles annealed at 530 °C for various durations are shown in figure 8. Extracted densities and diameters of the gold particles were plotted versus annealing time, as shown in figures 9 and 10, respectively. Clearly, the annealing time had the noticeable effect on the sizes of the nanoparticles. As shown in figure 10, the average diameter of the nanoparticles decreased slightly as annealing time increased, although the average values could be skewed by the samples we chose. However, the variance in size clearly decreased from a range of nearly 80 nm to about 45 nm. There did not appear to be a correlation between the annealing time and the density of the particles.

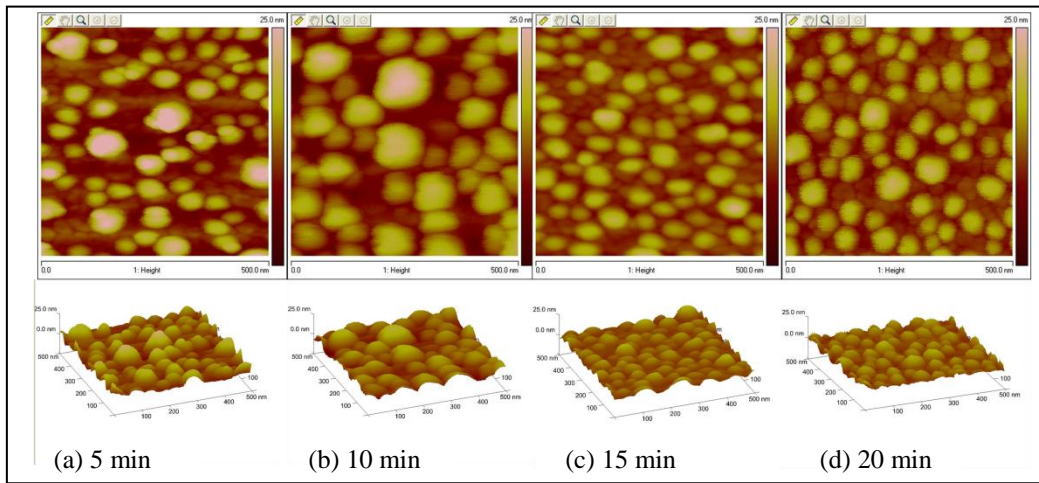


Figure 8. AFM images of gold nanoparticles with a 100-nm-thick initial layer and annealed at 530 °C for various times. Images were taken with a sample size of 500 nm x 500 nm and vertical scale of 25 nm, with the corresponding 3-D view below.

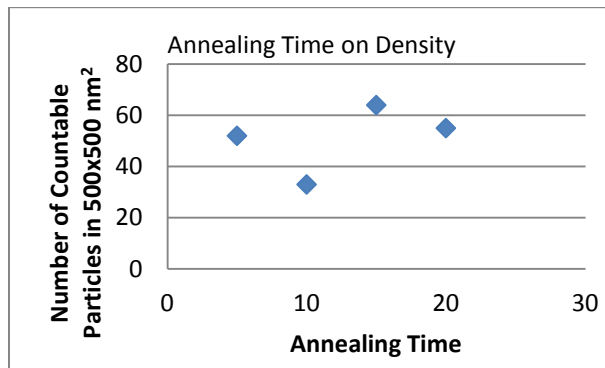


Figure 9. Densities of the gold particles as a function annealing time.

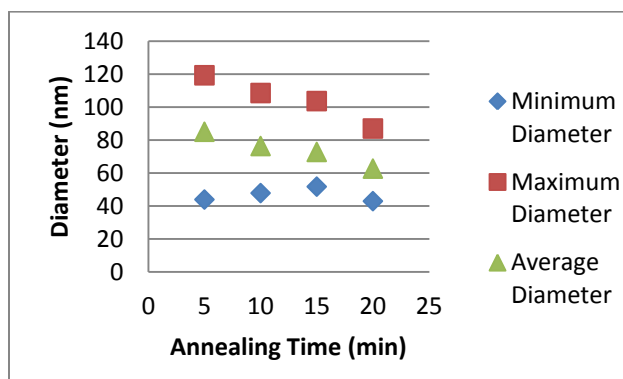


Figure 10. Diameters of the gold particles as a function annealing time.

4. Conclusions

In conclusion, we found that changing the thickness of the initial layer, the annealing temperature, and annealing time had some influence on the size of the nanoparticles, but did not clearly influence the density. The annealing time seemed to have the greatest effect, while the annealing temperature has the smallest effect. In general, annealing for longer times yields smaller particles with a smaller size distribution. However, the exact relationship between the growth parameters and the resulting properties is unclear. Due to time constraints, we could do multiple trials for only a few runs, and more trials for the other conditions are needed to confirm our results. Further runs with thicker layers and at higher and lower annealing temperatures and times could be helpful in illuminating the overall trend.

Although the AFM was helpful in producing 3-D images, the analyzing tools were not very accurate, which may have skewed our quantitative results. More experience with the AFM, more advanced image processing tools, or more scans could give us more accurate results.

For the purpose of forming nanobridges, we wanted the nanoparticles to be as dense and large as possible. Thus, an initial layer 100 nm thick yielded the largest nanoparticles, while annealing at 530 °C and 10 or 15 min yielded the densest particles.

5. References

1. Wagner, R. S.; Ellis, W. C. Vapor-Liquid-Solid Mechanism of Single Crystal Growth. *Applied Physics Letters* **1964**, 4(5), 89–90. doi:10.1063/1.1753975
2. Zakharov, N.; Werner, P.; Sokolov, L.; Gosele, U. Growth of Si whiskers by MBE: Mechanism and peculiarities. *Physica E* **2007**, 37, 148–152. doi:10.1016
3. Wojtowicz, T.; Janik, E.; Zaleszczyk, W.; Sadowski, J.; Karczewski, G.; DluZewski, P.; Petrouchik, A. MBE Growth and Properties of ZnTe- and CdTe-Based Nanowires. *Journal of the Korean Physical Society* **2008**, 53 (5), 3055–3063.

List of Symbol, Abbreviation, and Acronyms

3-D	three dimensional
AFM	atomic force microscope
Cd	cadmium
CdTe	cadmium telluride
H ₂ O	water
H ₂ O ₂	hydrogen peroxide
HCl	hydrochloric acid
HF	hydrogen fluoride
In	indium
MBE	molecular beam epitaxy
NH ₃ OH	ammonium hydroxide
RHEED	reflection high-energy electron diffraction
Se	selenium
SEM	scanning electron microscopy
Si	silicon
VLS	vapor-liquid-solid
ZnTe	zinc telluride

1 DEFENSE TECHNICAL
(PDF) INFORMATION CTR
DTIC OCA

2 DIRECTOR
(PDFS) US ARMY RESEARCH LAB
RDRL CIO LL
IMAL HRA MAIL & RECORDS MGMT

1 GOVT PRINTG OFC
(PDF) A MALHOTRA

5 DIRECTOR
(PDF) US ARMY RESEARCH LAB
RDRL SEE I
GLENN R. YU
HANS M GUO
YUANPING CHEN
PRIYALAL S WIJEWARNASURIYA
PARVEZ N UPPAL

INTENTIONALLY LEFT BLANK.